Available online at www.sciencedirect.com
ScienceDirect
Trans. Nonferrous Met. Soc. China 21(2011) 2358−2364
Transactions of Nonferrous Metals Society of China
www.tnmsc.cn

High strength magnesium alloy with α-Mg and W-phase processed by hot extrusion

YANG Wen-peng[1], GUO Xue-feng[2]

1. School of Materials Science and Engineering, Xi'an University of Technology, Xi'an 710048, China;
2. School of Materials Science and Engineering, Henan Polytechnic University, Jiaozuo 454003, China

Received 20 December 2010; accepted 26 April 2011

Abstract: Fine-grained Mg−6Zn−4Y alloy was prepared by an ingot metallurgy process with hot extrusion at 300 °C. The microstructure was studied by XRD, OM, SEM and TEM, and the tensile properties were tested at room temperature. The results show that the alloy is composed of α-Mg and W-phase. The microstructure of the as-extruded alloy has a bimodal grain size distribution. The fine grains with the mean size of 1.2 μm are formed by dynamic recrystallization. The coarse grains (about 23% in area fraction) are unrecrystallized regions which are elongated along extrusion direction. The engineering stress—strain curve shows a pronounced yield point. The ultimate tensile strength, yield strength, and elongation are (371±10) MPa, (350±5) MPa and (7±2)%, respectively. The high strengths are attributed to the fine-grained matrix structure enhanced by W-phase particles, nano-scaled precipitates, and strong basal plane texture.

Key words: Mg−6Zn−4Y alloy; extrusion; W-phase; high strength; yield phenomenon

1 Introduction

Mg-based alloys are attractive for many engineering structural applications owing to their low density and high specific strength [1]. However, Mg and most Mg alloys have hexagonal close-packed crystal structure that does not have sufficient slip systems; hence it is hard to increase their strengths and ductilities simultaneously. Recently, Mg alloys containing Zn and Y have attracted a great deal of attention as they have high strengths and reasonable ductilities [2−3]. In general, depending on the Zn/Y ratio ternary equilibrium phases in as-cast and rapidly solidified Mg−Zn−Y system include I-phase (Mg_3YZn_6), W-phase ($Mg_3Y_2Zn_3$), and long-period stacking order (LPSO) structures (including 6H, 14H and 18R etc) [4−5]. The alloys with the novel LPSO structures have excellent properties because the hard LPSO structures and the coherent LPSO/α-Mg interface can provide with high strength and fractural resistance to Mg alloys. As an example, Mg−2Y−1Zn (mole fraction, %) alloy strengthened by 6H LPSO structure consolidated at various temperatures from gas-atomized powder exhibits yield strengths of 480−610 MPa in company with elongations of 5%−16% at room temperature [6]. I-phase is a stable icosahedral quasicrystalline phase with high lattice symmetry. By far, five orientation relationships between I-phase and Mg matrix have been identified [7−8]. Each has strong interfacial properties due to the low interfacial energy. The Mg−Zn−Y alloys containing I-phase have yield strengths of 190−320 MPa and elongations of 15%−25% at room temperature after being processed by hot rolling and extrusion [2−3]. W-phase with face-centered cubic structure has weak adhesive force with Mg matrix due to their limited structural symmetry [9]. Nevertheless, the strengthening mechanisms for high strength Mg alloys containing W-phase have more possibilities except W-phase strengthening. The matrix grain size [10], texture [11] and volume fraction of strengthening particles [12] are perhaps also the key factors to strength and ductility. However, few reports investigated the effects of above factors on the mechanical properties. In this study, we report a high strength two-phase alloy containing α-Mg and W-phase, which was prepared by hot extrusion from as-cast Mg−6Zn−4Y ingot, and the

Foundation item: Project (50271054) supported by the National Natural Science Foundation of China; Project (20070700003) supported by the Doctorate Programs Foundation of Ministry of Education of China; Project (102102210031) supported by the Science and Technologies Foundation of Henan Province, China; Project (2010A430008) supported by the Natural Science Foundation of Henan Educational Committee of China

Corresponding author: YANG Wen-peng; Tel: +86-29-82314009; E-mail: wenpengy@gmail.com

DOI: 10.1016/S1003-6326(11)61020-0

strengthening mechanism is discussed.

2 Experimental

The as-cast alloy with the nominal composition of Mg−6Zn−4Y was prepared by melting Mg (99.9%), Zn (99.9%) and Mg−47%Y master alloy in an electric resistance furnace at 720 °C under Ar+SF_6 atmosphere. The ingots with a diameter of 52 mm and a length of 120 mm were prepared by pouring melt into graphite moulds.

The as-cast ingots were machined into rods with a diameter of 50 mm and a length of 50 mm for extrusion. Before extrusion, the billets and extrusion die were heated to 300 °C for 60 min in order to homogenize the temperature of the billets. The billets were extruded into bars with a diameter of 12 mm at an extrusion ratio of 17:1 and a ram speed of 1 mm/min.

The phase constitutions were analyzed by a Rigaku D/max-C X-ray diffraction (XRD) instrument with Cu K_α radiation. Metallographic specimen was polished to mirror and then etched using a solution of 0.5 mL nitric acid + 5 g picric acid + 10 mL acetic acid + 10 mL water + 100 mL alcohol. The specimen was examined by a Niko Epiphot optical microscope (OM). The grain size (d) was estimated using an image analysis software based on OM micrograph. During evaluation, over 2 000 grains were measured. The distribution of broken W-phase was observed using a JSM−6700F scanning electron microscope (SEM). Transmission electron microscopy (TEM) was employed to obtain detailed information about microstructure including features of strengthening particles and dislocations. TEM sample was cut from as-extruded bar along the extrusion direction (ED). The sample was twin-jet electron-polished to perforation, then ion-milled to remove oxide film with an ion accelerating voltage of 4 keV. TEM observation was carried out using a JEM−3010 operating at 300 kV.

Tensile specimen with a gauge length of 30 mm and a diameter of 6 mm was machined from the as-extruded bar along ED. Tensile tests were carried out using a HT2008 machine at a constant strain rate of 5×10^{-4} s^{-1} at room temperature.

3 Results

Figure 1 shows the XRD pattern of Mg−6Zn−4Y alloy. The alloy is mainly composed of α-Mg and W-phase. This result agrees well with the previous studies [4−5], in which it was found that the predominant intermetallic compound is W-phase when Zn/Y ratio is between 1 and 2.

Figure 2 shows the microstructures of as-extruded alloy on longitudinal section. The as-extruded alloy consists of fine equiaxed grains and some coarse grains (Fig. 2(a)). This kind of microstructure has typical bimodal grain size distribution and is commonly observed in the alloys extruded at relatively low temperatures [13]. According to the previous reports, the fine grains with an average grain size of 1.2 μm are attributed to the dynamic recrystallization (DRX). The coarse grains are the ones that did not undergo recrystallization, and kept the elongated form along ED with an aspect ratio of more than two order of magnitude and serrated boundaries. The area fraction of the unrecrystallized regions is measured to be about 23%.

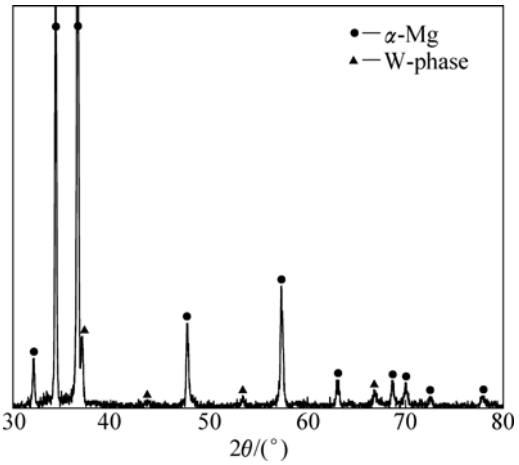

Fig. 1 XRD pattern of Mg−6Zn−4Y alloy

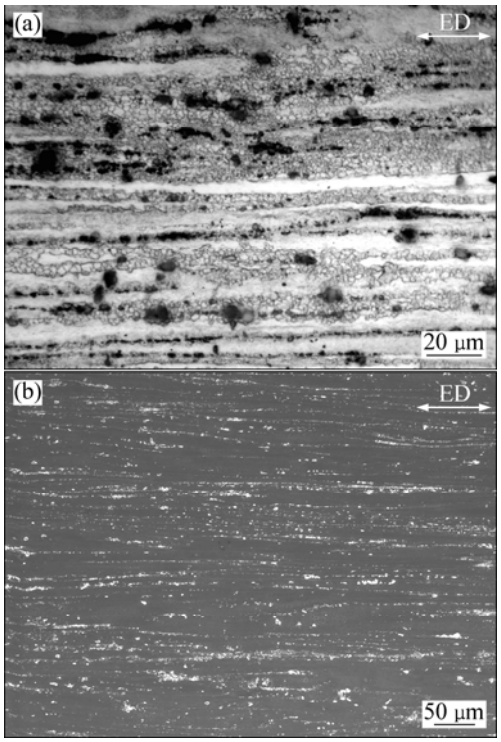

Fig. 2 Microstructures of as-extruded Mg−6Zn−4Y alloy: (a) OM micrograph showing fine recrystallized grains and elongated unrecrystallized grains; (b) SEM micrograph showing broken intermetallics

The dark regions in Fig. 2(a) are the broken W-phase particles formed during extrusion from grain boundary networks of the as-cast alloy. The SEM micrograph shown in Fig. 2(b) provides good contrast between the intermetallics and matrix. It is clear from Fig. 2(b) that the broken W-phase (white regions) particles are distributed as streamlines in parallel to ED. The area fraction of W-phase is measured to be about 6.7%.

Figure 3(a) shows a bright-field TEM image taken from the streamline region. The average grain size in this region is smaller than 1 μm. Most of grains are dislocation free; some grains containing high density of tangled dislocations are indicated by white arrows. W-phase particles with large size of 1.3 μm and small size of 50 nm are distributed in the matrix. The inset in Fig. 3(a) shows the selected area electron diffraction pattern of the W-phase recorded from [111] zone axis.

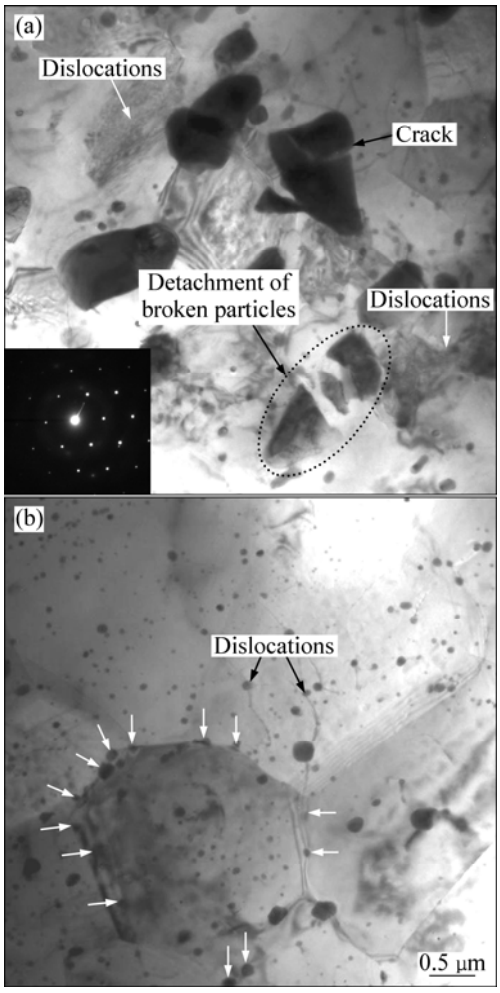

Fig. 3 TEM bright-field images of as-extruded Mg−6Zn−4Y alloy: (a) Taken from streamline region showing broken intermetallics and matrix microstructure (the inset is [111] selected area electron diffraction pattern taken from W-phase); (b) Taken from a region without large broken particles showing coarse grains and nano-scaled precipitates

The large particles are broken eutectic W-phase. The broken process can be deduced from the crack and detached particles, as indicated by the black arrow and dotted ellipse. The small particles are precipitates which mainly are dispersed along grain boundaries.

A bright-field TEM image taken from large-particle free region is shown in Fig. 3(b). The grains in this region are coarse in comparison with those in streamline regions. A large number of small particles of 50 nm are homogeneously dispersed within the matrix. Those precipitates distributed along grain boundaries (indicated by the white arrows) can pin grain boundaries movements and retard grain growth at elevated temperatures. Some dislocations locked by the small particles can be observed within the grains, as indicated by the black arrows.

The engineering stress — strain curves of as-extruded Mg−6Zn−4Y alloy consistently show pronounced yield points. A representative one is shown in Fig. 4. According to the engineering stress—strain curves, the yield strength (YS), ultimate tensile strength (UTS) and elongation (δ) are (350±5) MPa, (371±10) MPa and (7±2)%, respectively.

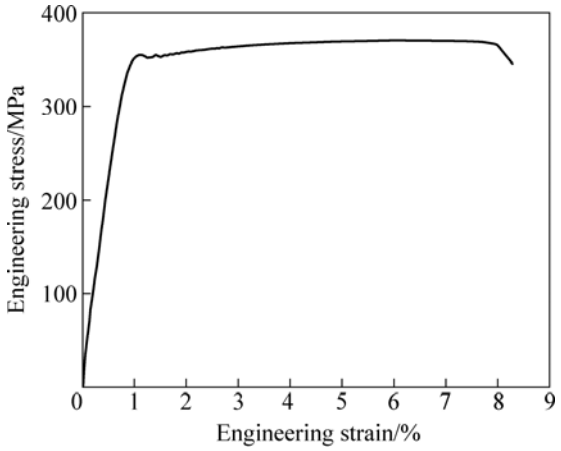

Fig. 4 Engineering stress — strain curve of as-extruded Mg−6Zn−4Y alloy

Figure 5 shows the tensile fracture of the as-extruded Mg−6Zn−4Y alloy. The fracture consists most of dimples and a few cleavage surfaces (Fig. 5(a)). The high magnification fractograph (Fig. 5(b)) reveals that the distribution of intermetallic particles on the fracture surface is not uniform. In some regions many particles crowd together, as indicated by the dotted circles. These regions are the streamline areas on the cross-sections, as shown in Fig. 2(b). It is reasonable to conclude from Fig. 5 that during tensile test the dislocations pile up around the strengthening particles and result in microvoids forming at the interfaces between the intermetallic particles and the matrix. Therefore, the microvoids initially derive from the

regions containing high density of particles, for example, the dotted circle regions as marked in Fig. 5(b), then the microvoids grow and coalesce into large cavities and finally result in fracture occurring.

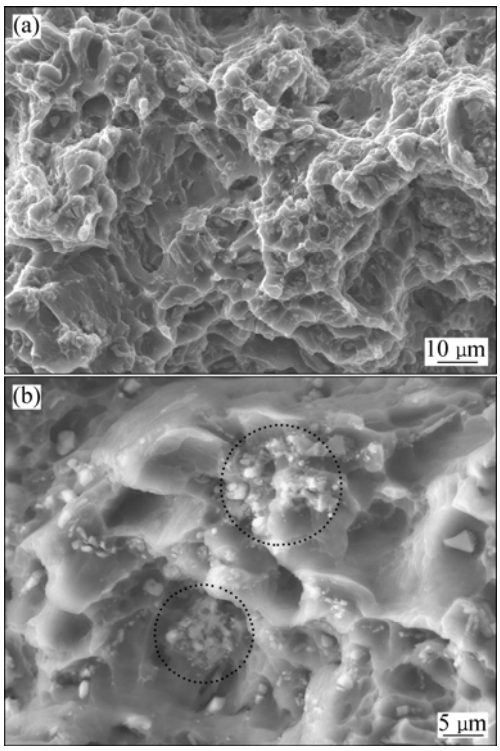

Fig. 5 SEM images of fracture surfaces of as-extruded Mg−6Zn−4Y alloy: (a) Surface morphology; (b) Distribution of strengthening particles

4 Discussion

4.1 Microstructure

Thermomechanical treatments are effective to: 1) refine matrix by DRX; 2) break intermetallic particles within grains and networks at grain boundaries, and make the strengthening particles well-distributed; 3) obtain uniform precipitates during hot working and following cooling process; and 4) form strong basal plane texture. It is suggested that microstructural refinement is much connected with processing parameters, such as wrought temperature, deformation ratio and deformation speed. Working with small deformation ratio and at low temperature, inadequate recrystallization is observed sometimes, and uniform microstructure is hard to be achieved. As shown in Fig. 2(a), the microstructure of as-extruded Mg−6Zn−4Y alloy consists of 23% unrecrystallized regions; these regions have serrated boundaries. This kind of microstructure is considered to be the result of discontinuous DRX. The nucleation of recrystallized grains originates from the regions with high density of dislocation and large lattice misorientation, because those regions store much energy needed for recrystallization. TEM observation found that at the initiation of hot deformation, the tangled dislocations focus on the original grain boundaries and the grain boundaries become wavy and corrugated [14]. Therefore, the recrystallized grains are firstly formed on the original grain boundaries by boundary bulging. As the strain is increased, more DRX grains are formed, and the original boundaries become more serrated. Since the coarser grains have larger grain boundary lengths, they have a great tendency to develop into serrated grain boundaries. Therefore, it can be concluded that the unrecrystallized grains are the residuals of original coarser grains. It was reported that the unrecrystallized grains have strong basal texture along ED [15]. However, they do not have enough stored energy to trigger recrystallization. As a consequence, the grains are deformed in shape, have large aspect ratio and conserve the coarse form as a whole.

In addition, the strengthening particles can pin and prevent the movement of dislocations which are tangled and stored around the strengthening particles. Hence, the W-phase particles distributed in the alloy could act as the nucleation sources of DRX. At the same time, the strengthening particles have strong pinning effect to prevent the growth of recrystallized grains (Fig. 3). Therefore, the strengthening particles dispersed in the matrix play an important role in refining process during hot deformation.

4.2 Tensile properties

In general, alloys containing W-phase are supposed to have low strengths due to weak interface bonding between the matrix and W-phase. However, in the present experiment, Mg−6Zn−4Y alloy containing W-phase exhibits high tensile strengths. In order to compare with the previous results, the data of Mg−Zn−Y(−Zr) and Mg−Zn−Gd alloys are summarized in Table 1. It is apparent from Table 1 that the strengths of Mg−6Zn−4Y alloy are higher than those of Mg−Zn−Y alloys, and are as high as those of Mg−2.3Zn−14Gd alloy which has ultrafine-grained matrix enhanced by 14H LPSO structure. It is emphasized that grain refinement is the main strengthening mechanism for Mg alloys. For Mg−6Zn−4Y alloy, in addition to the contribution of grain refinement, high volume fraction of W-phase and strong fiber texture have large contributions as well.

The interface between the W-phase and α-Mg is incoherent. Hence, the W-phase particles are hard to shear by dislocation during tension and have strong pinning effect on the moving of dislocation in comparison with the phase having coherent interface

Table 1 Tensile properties of Mg−6Zn−4Y alloy and previous data of Mg−Zn−Y and Mg−Zn−Gd alloys

Material	Phase	t_{EX}*/°C	d/μm	YS/MPa	UTS/MPa	δ/%
Mg−6.4Zn−1Y [16]	I-phase	250	10	213	321	18
Mg−5.53Zn−1.08Y−0.83Zr [11]	I-phase	390	8	200	345	10.8
Mg−5.47Zn−3.69Y−0.86Zr [17]	W-phase	390	4	216	318	12
Mg−6.4Zn−1Y [18]	I-phase	400	3	252	335	12
Mg−6.7Zn−1.4Y [2]	I-phase	210	1.0	315	337	16.8
Mg−2.3Zn−14Gd [19]	14H	350	0.5	345	380	6.9
Mg−6Zn−4Y	W-phase	300	1.2	350	371	7

*t_{EX} is the extrusion temperature

with the matrix. Thus, it is reasonable to conclude that materials containing W-phase also have high strengths.

At room temperature, the values of critical shearing stress for dislocation slip on $\{10\bar{1}0\}\langle 11\bar{2}0\rangle$ prismatic and $\{10\bar{1}2\}\langle 11\bar{2}0\rangle$ or $\{10\bar{1}2\}\langle 11\bar{2}0\rangle$ pyramidal systems are about 100 times larger than those on the $\{0001\}\langle 11\bar{2}0\rangle$ basal slip system in pure magnesium [3]. Hence, the basal slip system is the easiest system to be activated and play the dominant role in plastic deformation at room temperature or moderately elevated temperatures. The prismatic and pyramidal slip systems only can be activated at high temperatures [20] or with fine grain size smaller than 10 μm at room temperature [21]. According to the Schmid's law, when the slip plane and the slip direction are at 45° relative to the stress axis, a maximum Schmid factor occurs and the shearing stress on the slip system reaches the maximum. However, AZEEM et al [22] found that the elongated grains are aligned along $\langle 11\bar{2}0\rangle$ crystal direction with their ***c***-axis perpendicular (within ±5°) to ED, thus the Schmid factor values on $\{0001\}\langle 11\bar{2}0\rangle$ for the unrecrystallized grains are very low [23]. Furthermore, since the basal slip modes are restricted due to the strong fiber texture, the unrecrystallized regions may deform by twinning. The $\{10\bar{1}2\}\langle 10\bar{1}1\rangle$ twinning system is the easiest system to be activated. Unfortunately, it is not active when the tensile direction is parallel to the basal plane [24]. Therefore, these grains have high resistance against yielding during tensile test. The as-extruded Mg−6Zn−4Y alloy contains 23% unrecrystallized regions, which have a significant improvement on the yield strength.

4.3 Yield phenomenon

The engineering stress — strain curve for the as-extruded Mg−6Zn−4Y alloy shows a pronounced yield point, which is not often observed in Mg alloys. To the best of our knowledge, the earliest explanation about yield phenomenon was proposed by CLARK [25] in an Mg−Zn alloy. The yield point is attributed to the pinning effect on dislocations by β'_1 precipitates at initial state, which are nucleated previously along the dislocation lines. Recently, the yield phenomena have been observed in Mg−Zn−Y [10] and Mg−Zn−Y−Ce [26] alloys processed by powder metallurgy at consolidation temperatures below 300 °C. The alloys have fine grain sizes between 500 nm and 1.5 μm. Interestingly, when the wrought temperatures are above 300 °C, the yield phenomenon disappears. MORA et al [10] suggested that the yield phenomenon may be due to the weak texture of the alloy extruded at low temperatures because the stress required for twinning increases with decreasing grain size more rapidly than the stress required to activate slip. But this yield phenomenon associated with the inhibition of twinning only maybe occurs in compression. Further, the yield phenomenon is rarely observed in as-extruded alloys with typical basal texture prepared from as-cast ingot.

The present authors suggest that the yield phenomenon could be related to the interaction of the residual dislocations with the strengthening particles. At high extrusion temperatures, the motion of dislocations is active and dislocations can easily move to grain boundaries and be absorbed, thus the DRX grains are dislocation free. However, at low extrusion temperatures, the motion of dislocations is not so active; some dislocations remain in grains and are pinned by the strengthening particles, as shown in Fig. 3(b). As a result, at the initial stage of tensile test, excess breakaway stress is required to overcome the pinning effects of the strengthening particles. When the dislocations break through the influence of strengthening particles, slip could occur at low stress, and the corresponding process on the stress—strain curve is the yield phenomenon.

5 Conclusions

1) Mg−6Zn−4Y alloy is mainly composed of α-Mg and W-phase, and the area fraction of W-phase is about 6.7%. The alloy extruded at 300 °C is not completely

recrystallized, which has a bimodal grain size distribution. The average size of DRX grains is 1.2 μm, and the area fraction of the unrecrystallized regions is about 23%. In addition, the large particles of 1.3 μm and fine precipitates of 50 nm are distributed in the matrix.

2) The yield strength, ultimate tensile strength and elongation of the as-extruded Mg−6Zn−4Y alloy are (350±5) MPa, (371±10) MPa and (7±2)%, respectively. Besides the contribution of grain refinement, the broken W-phase particles, nano-scaled precipitates, and strong basal texture are considered to have significant improvements on the strengths.

3) The yield phenomenon, which was rarely reported, was observed in the engineering stress—strain curve of the as-extruded Mg−6Zn−4Y alloy. It is suggested that the yield phenomenon is attributed to the pinning effect of strengthening particles on the residual dislocations at initial stage of tensile test.

References

[1] LI Yong-jun, ZHANG Kui, LI Xing-gang, MA Ming-long, WANG Hai-zhen, HE Lan-qiang. Influence of extrusion on microstructures and mechanical properties of Mg−5.0Y−7.0Gd−1.3Nd−0.5Zr [J]. The Chinese Journal of Nonferrous Metals, 2010, 20(9): 1692−1697. (in Chinese)

[2] SOMEKAWA H, SINGH A, MUKAI T. High fracture toughness of extruded Mg−Zn−Y alloy by the synergistic effect of grain refinement and dispersion of quasicrystalline phase [J]. Scripta Materialia, 2007, 56(12): 1091−1094.

[3] MÜLLER A, GARCÉS G, PÉREZ P, ADEVA P. Grain refinement of Mg−Zn−Y alloy reinforced by an icosahedral quasicrystalline phase by severe hot rolling [J]. Journal of Alloys and Compounds, 2007, 443(1−2): L1−L5.

[4] HUANG Z, LIANG S, CHEN R, HAN E. Solidification pathways and constituent phases of Mg−Zn−Y−Zr alloys [J]. Journal of Alloys and Compounds, 2009, 468(1−2): 170−178.

[5] ZHU Y, MORTON A, NIE J. The 18R and 14H long-period stacking ordered structures in Mg−Y−Zn alloys [J]. Acta Materialia, 2010, 58(8): 2936−2947.

[6] KAWAMURA Y, HAYASHI K, INOUE A, MASUMOTO T. Rapidly solidified powder metallurgy $Mg_{97}Zn_1Y_2$ alloys with excellent tensile yield strength above 600 MPa [J]. Materials Transactions, 2001, 42(7): 1172−1176.

[7] SINGH A, TSAI A. A new orientation relationship OR4 of icosahedral phase with magnesium matrix in Mg−Zn−Y alloys [J]. Scripta Materialia, 2005, 53(9): 1083−1087.

[8] SINGH A, WATANABE M, KATO A, TSAI A. Twinning and the orientation relationships of icosahedral phase with the magnesium matrix [J]. Acta Materialia, 2005, 53(17): 4733−4742.

[9] ZHANG Y, ZENG X, LIU L, LU C, ZHOU H, LI Q, ZHU Y. Effects of yttrium on microstructure and mechanical properties of hot-extruded Mg−Zn−Y−Zr alloys [J]. Materials Science and Engineering A, 2004, 373(1−2): 320−327.

[10] MORA E, GARCÉS G, OÑORBE E, PÉREZ P, ADEVA P. High-strength Mg−Zn−Y alloys produced by powder metallurgy [J]. Scripta Materialia, 2009, 60(9): 776−779.

[11] XU D, LIU L, XU Y, HAN E. Effect of microstructure and texture on the mechanical properties of as-extruded Mg−Zn−Y−Zr alloys[J]. Materials Science and Engineering A, 2007, 443(1−2): 248−256.

[12] LEE J Y, LIM H K, KIM D H, KIM W T, KIM D H. Effect of volume fraction of quasicrystal on the mechanical properties of quasicrystal-reinforced Mg−Zn−Y alloys [J]. Materials Science and Engineering A, 2007, 449−451: 987−990.

[13] GUO Yan-yan, LIN Zhi-xun, JIANG Hai-yan, WU Gao-hua. Effect of extrusion process on microstructure and mechanical properties of ME20M magnesium alloy [J]. The Chinese Journal of Nonferrous Metals, 2010, 20(8): 1147−1454. (in Chinese)

[14] ZHANG Y, ZENG X, LU C, DING W. Deformation behavior and dynamic recrystallization of a Mg−Zn−Y−Zr alloy [J]. Materials Science and Engineering A, 2006, 428(1−2): 91−97.

[15] XU D, LIU L, XU Y, HAN E The relationship between macro-fracture modes and roles of different deformation mechanisms for the as-extruded Mg−Zn−Zr alloy [J]. Scripta Materialia, 2008, 58(12): 1098−1101.

[16] SINGH A, NAKAMURA M, WATANABE M, KATO A, TSAI A. Quasicrystal strengthened Mg−Zn−Y alloys by extrusion [J]. Scripta Materialia, 2003, 49(5): 417−422.

[17] XU D, LIU L, XU Y, HAN E. The influence of element Y on the mechanical properties of the as-extruded Mg−Zn−Y−Zr alloys [J]. Journal of Alloys and Compounds, 2006, 426(1−2): 155−161.

[18] SINGH A, WATANABE M, KATO A, TSAI A. Microstructure and strength of quasicrystal containing extruded Mg−Zn−Y alloys for elevated temperature application [J]. Materials Science and Engineering A, 2004, 385(1−2): 382−396.

[19] YAMASAKI M, ANAN T, YOSHIMOTO S, KAWAMURA Y. Mechanical properties of warm-extruded Mg-Zn-Gd alloy with coherent 14H long periodic stacking ordered structure precipitate [J]. Scripta Materialia, 2005, 53(7): 799−803.

[20] GALIYEV A, KAIBYSHEV R, GOTTSTEIN G. Correlation of plastic deformation and dynamic recrystallization in magnesium alloy ZK60 [J]. Acta Materialia, 2001, 49(7): 1199−1207.

[21] KOIKE J, KOBAYASHI T, MUKAI T, WATANABE H, SUZUKI M, MARUYAMA K, HIGASHI K. The activity of non-basal slip systems and dynamic recovery at room temperature in fine-grained AZ31B magnesium alloys [J]. Acta Materialia, 2003, 51(7): 2055−2065.

[22] AZEEM M, TEWARI A, MISHRA S, GOLLAPUDI S, RAMAMURTY U. Development of novel grain morphology during hot extrusion of magnesium AZ21 alloy [J]. Acta Materialia, 2010, 58(5): 1495−1502.

[23] HOMMA T, MENDIS C, HONO K, KAMADO S. Effect of Zr addition on the mechanical properties of as-extruded Mg−Zn−Ca−Zr alloys [J]. Materials Science and Engineering A, 2010, 527(9): 2356−2362.

[24] GARCÉS G, MÜLLER A, OÑORBE E, PÉREZ P, ADEVA P. Effect of forging on the microstructure and mechanical properties of Mg−Zn−Y alloy [J]. Journal of Materials Processing Technology, 2008, 206(1−3): 99−105.

[25] CLARK J. Transmission electron microscopy study of age hardening in a Mg−5wt.%Zn alloy [J]. Acta Materialia, 1965, 13(12): 1281−1289.

[26] GUO X, SHECHTMAN D. Reciprocating extrusion of rapidly solidified Mg−6Zn−1Y−0.6Ce−0.6Zr alloy [J]. Journal of Materials Processing Technology, 2007, 187−188: 640−644.

热挤压高强度 Mg-6Zn-4Y 合金

杨文朋[1]，郭学锋[2]

1. 西安理工大学 材料科学与工程学院，西安 710048；
2. 河南理工大学 材料科学与工程学院，焦作 454003

摘　要：通过铸造和 300 °C 热加压制备细晶 Mg−6Zn−4Y 合金，利用 XRD、OM、SEM 和 TEM 研究合金组织，并测试其室温拉伸性能。结果表明，合金主要由 α-Mg 和 W 相两相组成，挤压态合金具有双峰晶粒尺寸分布；细小晶粒为动态再结晶晶粒，平均尺寸为 1.2 μm；粗大晶粒(占面积分数的 23%)为未再结晶区域，并沿挤压方向被拉长。合金的极限抗拉强度、屈服强度和伸长率分别为(371±10) MPa，(350±5) MPa 和(7±2)%，其工程应力—应变曲线有明显的屈服点。合金高强度归因于晶粒细化和 W 相、纳米沉淀颗粒及强基面织构的增强作用。

关键词：Mg−6Zn−4Y 合金；挤压；W 相；高强度；屈服现象

(Edited by YUAN Sai-qian)